

2011

# Numerical Modeling of Extrusion Welding in Magnesium Alloys

Yan Xu

*Lehigh University*

Follow this and additional works at: <http://preserve.lehigh.edu/etd>

---

## Recommended Citation

Xu, Yan, "Numerical Modeling of Extrusion Welding in Magnesium Alloys" (2011). *Theses and Dissertations*. Paper 1271.

This Thesis is brought to you for free and open access by Lehigh Preserve. It has been accepted for inclusion in Theses and Dissertations by an authorized administrator of Lehigh Preserve. For more information, please contact [preserve@lehigh.edu](mailto:preserve@lehigh.edu).

**Numerical Modeling of Extrusion Welding in Magnesium Alloys**

by

Yan Xu

Presented to the Graduate and Research Committee

of Lehigh University

in Candidacy for the Degree of

Master of Science

in

Mechanical Engineering and Mechanics

Lehigh University

August, 2011

**Copyright by Yan Xu**

August, 2011

This thesis is accepted and approved in partial fulfillment of the requirements for the Master of Science.

---

Date

---

Thesis Advisor  
Dr. Wojciech Z. Misiolek

---

Chairperson of Department  
Dr. D. Gary Harlow

## **ACKNOWLEDGEMENTS**

I would like to thank the following organizations and individuals for their support and help in this research work. Financial support from the United States Council for Automotive Research (USCAR) (contract # 07-1864) the part of the performed research is appreciated. I want to thank the Loewy Family Foundation for their support through the Loewy Graduate Fellowship at Lehigh University. I also want to thank Lehigh University Mechanical Engineering and Mechanics Department for providing me the teaching assistance fellowship in the last semester of this work. It was not only a financial aid but also meaningful work experience which will serve me very well in the future.

I also want to express my gratitude to my advisor Dr. Wojciech Z. Misiolek who gave me phenomenal guidance throughout the entire project. In addition, I want to thank all the members of Institute for Metal Forming in Lehigh University, thank you for your help, support, and advices.

This work would have been much more difficult to complete without the DEFORM software training and technical support from the Scientific Forming Technologies.

At last, I would like to thank my parents Chunrong Ma and Quanxi Xu for their support and love over the time of my education for MS degree.

# TABLE OF CONTENTS

<b>CERTIFICATE OF APPROVAL.....</b>	<b>ii</b>
<b>ACKNOWLEDGEMENTS.....</b>	<b>iii</b>
<b>LIST OF FIGURES.....</b>	<b>vi</b>
<b>LIST OF TABLES.....</b>	<b>ix</b>
<b>ABSTRACT.....</b>	<b>1</b>
<b>1. Introduction.....</b>	<b>2</b>
1.1 Extrusion.....	2
1.1.1 Extrusion in Everyday Life.....	4
1.1.2 Extrusion in Engineering.....	6
1.2 Magnesium Alloys.....	8
1.3 Extrusion Welding.....	12
1.4 Extrusion Wilding Criteria.....	14
1.5 Numerical Modeling and Simulation.....	15
1.6 Limited Capabilities of DEFORM™.....	18
<b>2. Physical Experiment and Numerical Simulation.....</b>	<b>19</b>
2.1 “Double Hat” Extrusion Industrial Trail.....	19
2.2 Numerical Simulation - DEFORM™ 2D.....	22
2.2.1 “Pressure Plate” Simulation Method.....	22
2.3 Numerical Simulation with DEFORM™ 3D.....	29
<b>3. Results and Analysis.....</b>	<b>30</b>
3.1 Validation of the Simulation Results.....	30

3.2 Result and Analysis of DEFORM™ 2D Simulation.....	30
3.2.1 Fixed Pressure Plate.....	31
3.2.2 Flowing Pressure Plate.....	33
3.3 Result and Analysis of DEFORM™ 3D Simulation.....	37
<b>4. Conclusion.....</b>	<b>39</b>
<b>5. Further Work.....</b>	<b>40</b>
<b>6. References.....</b>	<b>43</b>
<b>7. VITA.....</b>	<b>45</b>

## LIST OF FIGURES

Figure 1. Typical tooling arrangement of extrusion process [2]. .....	3
Figure 2. Extrusion in everyday life: extruded Aluminum window profiles .....	5
Figure 3. Extrusion in everyday life: extruded Aluminum door profiles. ....	6
Figure 4. Space frame construction of Audi A8.....	7
Figure 5. Hexagonal close packed (HCP) structure of Magnesium. ....	9
Figure 6. The porthole extrusion die [6].....	13
Figure 7. Steps in port-hold die extrusion. a: Forward extrusion; b: Sideways extrusion; c: Multiple voids filling; d: Extrudate completion [7].....	13
Figure 8. Extrusion welding seam in: (a) DEFORM™ 2D simulation and (b) [15] DEFORM™ 3D simulation.....	19
Figure 9. “Double-Hat” extrudate. ED: Extrusion Direction, ND: Normal Direction, TD: Transverse Direction.[5]. ....	20
Figure 10. "Double Hat" extrusion die used in industrial trials.....	20
Figure 11. Location of welds within “Double Hat” profile.....	21
Figure 12. Pressure Plate in DEFORM™ 2D simulation: (a) Fixed Pressure Plate. (b) Flowing Pressure Plate. ....	22
Figure 13. Flow stress curves of AZ31 alloy generated by DEFORM™ for: (a) 300°C and (b) 500°C.....	27
Figure 14. Fixed Pressure Plate simulation showing Effective Stress distribution . The marked regions are: dead metal zone behind mandrel (DMZM), effective welding chamber (EWCH) and bearing land of the die (BL) . ....	28
Figure 15. Flowing Pressure Plate simulation showing Effective Stress distribution..	28
Figure 16. Extrusion simulation with Fixed Pressure Plate as marked with arrow in DEFORM™ 3D showing Effective Stress distribution: (a) Start of the simulation (b) Metal streams in contact with the fixed pressure plate. ....	29



Figure 17. Effective Stress along extrusion weld with the increase of the distance to the bottom of mandrel. The marked regions represent: dead metal zone behind mandrel (DMZM), effective welding chamber (EWCH) and bearing land of the die (BL). ..... 32

Figure 18. Normal Pressure along extrusion as the function of the distance to the bottom of mandrel. The marked regions represent: dead metal zone behind mandrel (DMZM), effective welding chamber (EWCH) and bearing land of the die (BL). ..... 32

Figure 19. Time vs. displacement of the flowing pressure plate. The marked regions are: dead metal zone behind the mandrel (DMZM), effective welding chamber (EWCH) and bearing land of the die (BL). ..... 33

Figure 20. Effective stress data of the flowing pressure plate along extrusion weld as the function of the distance to the mandrel tip. Marked regions are: dead metal zone behind the mandrel (DMZM), effective welding chamber (EWCH) and bearing land of the die (BL). ..... 34

Figure 21. Polynomial curve fit of effective stress data of the flowing pressure plate. The marked regions are: dead metal zone behind the mandrel (DMZM), effective welding chamber (WCH) and bearing land of the die (BL). ..... 35

Figure 22. Normal Pressure data of the flowing pressure plate along extrusion weld as the function of the distance to the mandrel tip. The marked regions are: dead metal zone behind the mandrel (DMZM), effective welding chamber (EWCH) and bearing land of the die (BL). ..... 35

Figure 23. Polynomial curve fit of normal pressure data of the flowing pressure plate. The marked regions are: dead metal zone behind the mandrel (DMZM), effective welding chamber (EWCH) and bearing land of the die (BL). ..... 36

Figure 24. Integration of  $P/\sigma$  as the function of the distance to the mandrel tip. The marked regions are: dead metal zone behind the mandrel (DMZM), effective welding chamber (EWCH) and bearing land of the die (BL). ..... 36

Figure 25. Distribution of effective stress on fixed pressure plate of DEFORM™ 3D simulation. ..... 38

Figure 26. Effective stress data of the fixed pressure plate in DEFORM™ 3D simulation. The marked regions are: dead metal zone behind the mandrel

(DMZM), effective welding chamber (EWCH) and bearing land of the die  
(BL). .....38

## LIST OF TABLES

Table 1. Typical Chemical Compositions (wt%, bal Mg) For AZ31 and AM30 Alloys [5]. .....	12
Table 2. Extrusion Trail Process Parameters.....	21
Table 3. Details for Two Types of the Pressure Plate. ....	23
Table 4. Initial Settings for the DEFORM <sup>TM</sup> 2D Pressure Plate Simulation. ....	24

## **ABSTRACT**

Solid-state welding takes place during the extrusion of hollow shapes and tubes made from selected metals such as aluminum and magnesium and their alloys. In this thesis, an industrial extrusion trial with the extrudate of the "Double Hat" hollow shape has been examined. The process parameters of this trial have been employed into finite element simulation as initial settings then. DEFORM<sup>TM</sup> is one of the most frequently used FEM software packages to analyze the metal flow in deformation processes. This software has been used as the main tool of the simulations for this work. However, it has some limitations while applied to study the extrusion welding. Both of the 2D and 3D versions of DEFORM<sup>TM</sup> cannot determine if extrusion welding takes place in a port-hole die. This limitation is a result of a lack of ability to transfer the localized deformation conditions to a judgment about a good or poor weld. In the meantime, the collection of the information about localized state variables in the welds is inaccurate. In this study, a new modeling method has been proposed to obtain the localized information at the extrusion welding seam. A so-called pressure plate was virtually inserted in the position of the extrusion welding seam, which plays a role of a sensor and has been recording all the information at the given seam during the entire extrusion process. Analytical methods have been utilized to study the data collected from this sensor to evaluate the probability of the formation of the sound extrusion welding seam. The generated results have been used to verify Plata & Piwnik extrusion welding criterion and can be implemented into existing extrusion models to achieve better prediction of weld integrity.

# **1. Introduction**

## **1.1. Extrusion**

The extrusion of metals is a process in which a billet usually heated to an elevated temperature is pressed by a punch at high pressure through a die of the desired shape. The die can be one or multi-orifices. The art of extrusion was firstly introduced to the stage of industry in nineteenth century. Since the low capacity of extrusion press, this technology was applied in very narrow range. From the start of the twentieth century, rapid developments of extrusion process gave this art wider application and better production quality. Nowadays, this approach has been mainly used for the production of bars, wires, tubes and sections mainly in Aluminum, Copper as well as Magnesium alloys [1]. The extrusion process has two main advantages over other manufacturing techniques: (1) it has good capability to create very complex cross-section shapes; (2) the product of extrusion process has an excellent surface finish. During a typical extrusion process, the billet of certain material is deformed under a compressive state. The extrusion process is able to achieve large deformation in one production step with relatively low cracking risk. The key factor extrusion ratio (also called die ratio in some literatures) is defined with the ratio of the billet cross-section area to that of the extrudate. The extrusion ratio is usually within the range 10 to 100 for most extrusion cases. Another important factor of extrusion is temperature. Extrusion is normally carried out at relatively high temperature: between 400 to 500°C for Aluminum alloys, between 300 to 600 °C for Magnesium alloys, between 600 to 900 °C for Copper alloys and up to 1200 °C for stainless steels and special materials. In Figure 1, it is showing the typical tooling arrangement of extrusion process.

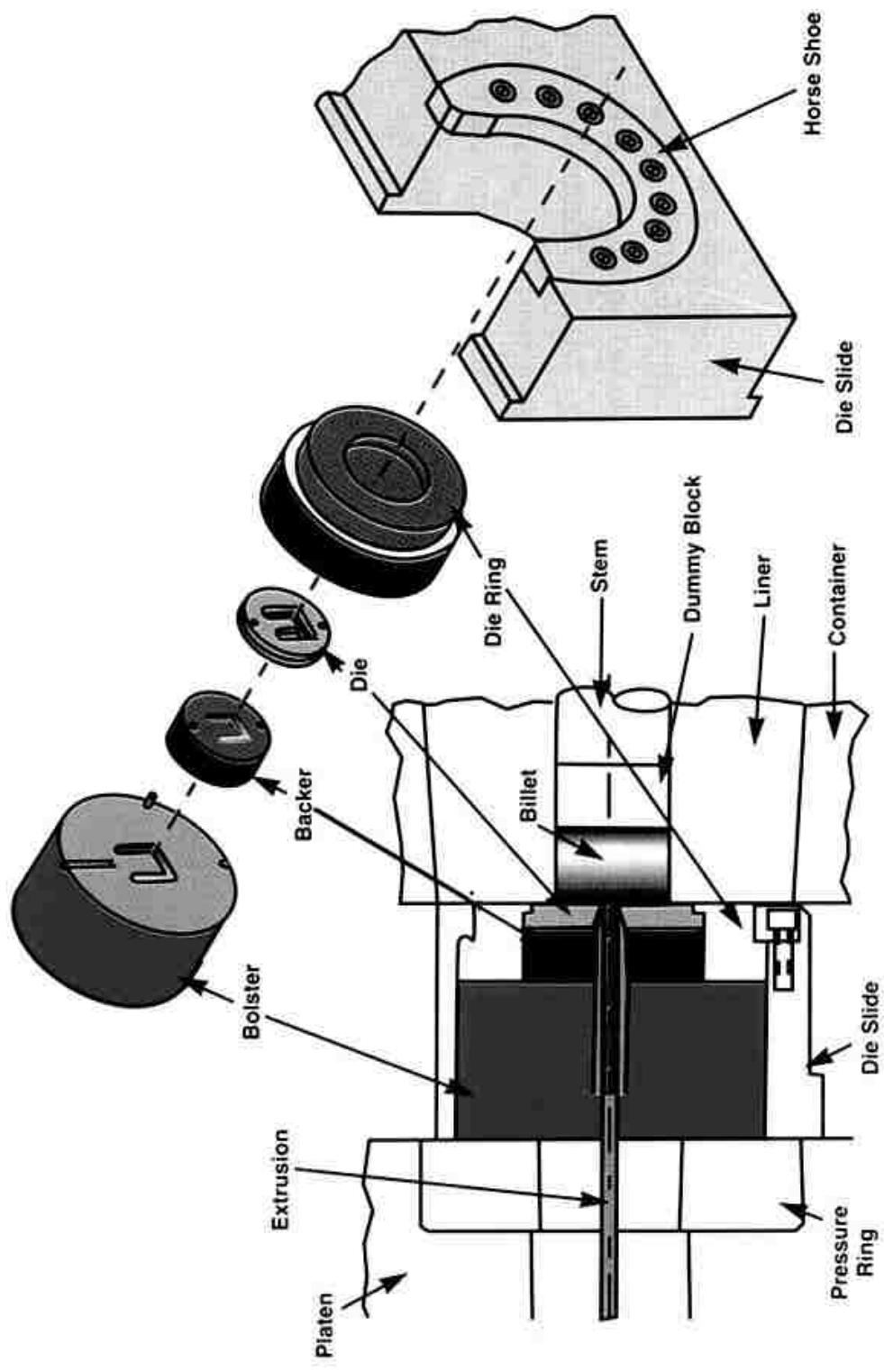


Figure 1. Typical tooling arrangement of extrusion process [2]

The extrusion is classified into hot-working process category, which is utilized to produce semi-finished products in the form of bar, strip, solid section, tube and hollow section. Compare with other hot-working processes, the biggest advantage of extrusion is the high mean compressive stresses in the deformation zone of the container of extrusion tooling. During the extrusion process, the material is pushed in and then extruded through the shape-forming chamber of the extrusion die (Figure 1). The high mean compressive stresses enable materials be processed with higher strain into much more complex shapes than any other forming processes, for instance the rolling process which has limited workability [1]. Today, the main application area of extrusion is production of hollow and semi-hollow sections. Under the desired deformation conditions, the nonferrous metals and their alloys such as Tin, Lead as well as Magnesium and Aluminum can exhibit good weldability during extrusion process. The tooling can withstand elevated extrusion temperatures as required hence enable the billet to be divided into several metal streams by the extrusion die, and then welded within the welding chamber to form tubes as well as hollow and semi-hollow sections. Billet-to-billet extrusion enables the transverse extrusion welding to take place between each two billets. Therefore, producing the long length tubes, for example, Aluminum alloy heat exchanger tubes and Tin-Lead alloy multi-core solders, has been achieved with great productivity.

### **1.1.1. Extrusion in Everyday Life**

The manufacture of Aluminum sections is the main application of extrusion in Aluminum alloys for everyday life use. Nowadays, extrusions of Aluminum alloys

which are used as a semi-finished product in people's life have the biggest application amount compare with other materials [1]. As the main extrusion material for everyday life use, Aluminum alloys have both economical and environmental advantages: favorable materials properties, good modulus of elasticity, low density, good surface quality, good dimensional accuracy and easy to recycle. The extruded Aluminum alloys are mainly utilized as the frames of doors and windows in commercial and residential housing. From the middle of 1900s, people's demand of building began expanding. As a result, the need of building elements including windows and doors obtained sharp increase simultaneously. Over the years, because of attractive surface finish and good corrosion properties, extruded aluminum sections has gained a large market and become one of the most important members of building elements.



Figure 2. Extrusion in everyday life: extruded Aluminum window profiles



Windows and doors have major influence on domestic quality as well as the energy efficiency of the building [1]. After the energy crisis toward the middle of the 1970s, a lot of changes has been happening in the design principle of windows and doors due to the ideas of thermal insulation and sound insulation have to be taken into consideration. Consequently, Aluminum extrusions are naturally the best suited candidate for the design with these new features, because of their good strength with low weight and the enormous possibility of complex section geometry. These advantages also gives architects more than enough room to think and create. Figures 2 and 3 are showing the extruded Aluminum window profiles and door profiles.



Figure 3. Extrusion in everyday life: extruded Aluminum door profiles

### **1.1.2. Extrusion in Engineering**

The advantages of Aluminum extrusions: favorable materials properties and modulus of elasticity, low density, good surface quality, good dimensional accuracy

and easy to recycle have attracted huge interest of engineers. The transition of Aluminum extrusion from the productions for everyday life to engineering world had become very natural. The peak point of this important technology transition is the Audi A8 and Audi A2 with the space frame construction of Alcoa. These two cars have the bodies entirely made of 6xxx Aluminum alloys. The sections assembled into the space frame are produced with extrusion. The principle of this construction is illustrated in Figure 4.

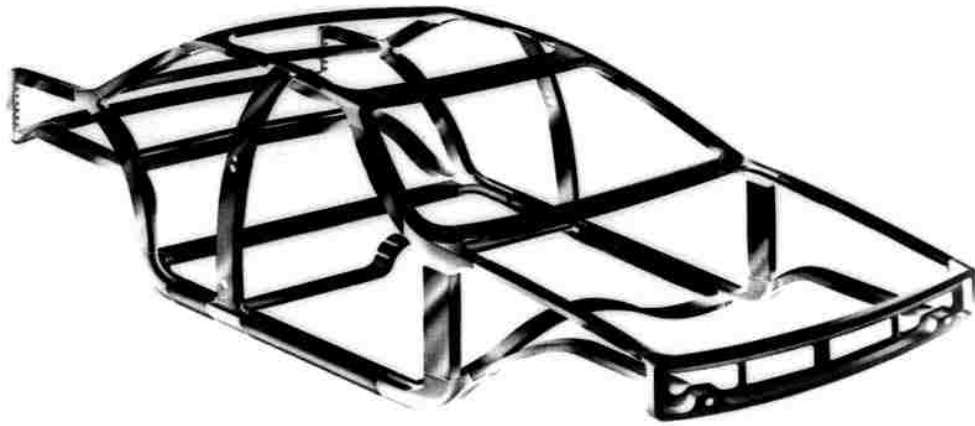


Figure 4. Space frame construction of Audi A8

Since the rapid developments of material science and alloy technique, the number of material candidate for extrusion is increasing continuously. Extrusions of Copper alloys are used to produce bar, wire, section and tube with simple cross-section and thicker wall, because it has relatively more severe thermal loading on tooling in the range of 600 to 900 °C extrusion temperature. Productions of extruded Titanium alloys are mainly applied in aircraft, spacecraft and rockets due to its light weight under

required thermo-mechanical loading. As mentioned before, extrusions of 6xxx Aluminum alloys are used widely in both everyday life and engineering. In addition, Aluminum Alloys 2xxxx (major alloying element is Copper) and 7xxxx (major alloying element is Zinc) have been applied widely in the aircraft industry for long time, due to their very high strength, excellent machinability and heat treatability. In this study, a Magnesium alloys AZ31 was selected because of its good properties and characteristics. The details about this material will be discussed in the following session.

## **1.2. Magnesium Alloys**

This work is part of the project where Magnesium alloys are proposed as structure components in automobiles. There is an increasing need to develop fabrication technologies for lightweight components, which are of interest in automobile industry due to a need to lower vehicles' mass in order to increase their mileage. Magnesium and its alloys is one of the material candidates because of its outstanding characteristics. A brief summary on the material properties of Magnesium has been obtained as following, according to the ASM handbook [3]. Magnesium is the third most commonly used structural metal, following Iron and Aluminum. It has great physical properties: approximately two-thirds the density of aluminum ( $\rho_{Mg} = 1.74\text{g/cm}^3$ ), high strength, good weldability, and good damping capacity. And in terms of the crystal structure, as shown in Figure 5, Magnesium has a hexagonal close packed (HCP) structure with a c/a ratio of 1.623. It is a very good crystal structure because the ideal close packing value of metal is 1.633, which is very close with the

value of Magnesium. If the deformation process takes place at ambient temperature, the plastic deformation is limited to the basal slip system. But if the process is performed at elevated temperature, prismatic slip will be also activated and therefore it will enhance the workability of Magnesium alloys. In comparison to other metals with different crystal structures the HCP structure has limited ductility because of lower number of slip systems (three for HCP versus twelve for FCC and BCC). As a result, Magnesium is less ductile than the FCC and BCC metals and alloys. Moreover, Magnesium alloys do easily corrode, thus all of them require special working atmosphere ( $\text{SO}_2$  gas) for casting and heat treatment. Protective coatings to prevent oxidation are necessary. Consequently, two major shortcomings of Mg alloys, limited formability and low corrosion resistance are the biggest obstacles in their applications.

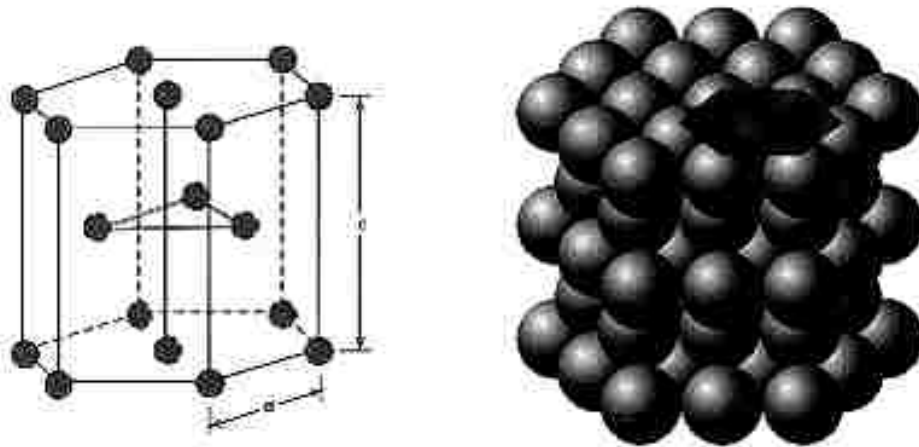


Figure 5. Hexagonal close packed (HCP) structure of Magnesium

Magnesium alloys are mixtures of magnesium with other metals. The common alloying elements are: Aluminum, Zinc, Manganese, Silicon, Copper, rare earths and Zirconium. As mentioned before, Magnesium alloys have a hexagonal lattice structure,

which is influencing the essential properties of these alloys. Plastic deformation of the hexagonal lattice is of more complexity than in cubic latticed metals such as Aluminum, Copper and Steel. Therefore Magnesium alloys were typically used as cast alloys in very beginning, but studies on extrusion of Magnesium alloys has been attracting increasing interest of engineers nowadays.

During the wrought process of Magnesium alloys, each alloying addition has specific role on changing the properties and characteristics of the alloys. A brief summary of the role of alloying elements in Mg alloys is available in literature [3]. According to the current studies, most wrought magnesium alloys are built on the foundation of Mg-Al-Zn-Mn system. Magnesium alloys in this category contain between 0 and 8% Aluminum component to maintain the strength under room temperature. Alloys in this group for common use are including M1A, AZ10A, AZ31B, AZ31C, AZ61A, and AZ80A. Furthermore, if Aluminum is added as the major alloying element, the Magnesium alloys will have improved strength, ductility, and resistance to atmospheric corrosion. Zinc is usually added to obtain additional strength and also can strengthen saltwater corrosion resistance when heavy-metal, Copper, Iron, and Nickel are controlled to low limits. In the same time, Manganese is another important alloying element for Magnesium alloys to control the corrosion properties. And if greater ductility and fracture toughness are required in some cases, a series of high-purity alloys with reduced Aluminum contents are proper choices. Examples are AM60A, AM60B, AM50A, and AM20. Within these Magnesium alloys, the amounts of  $Mg_{17}Al_{12}$  particles are declined around the grain boundaries in order to obtain better properties. Consequently, these Magnesium alloys are used for

automotive parts, including wheels, seat frames, and steering wheels etc. in industry today.

However, in terms of the wrought magnesium alloys on the Mg-Al system, they have a big limitation. When the working temperature is above 120 to 130 °C (250 to 265 °F), the mechanical properties of both the AZ group and the AM group of Magnesium alloys decrease very quickly. The reason for that is, the grain-boundary sliding is the key makes Magnesium alloys undergo creep, but the  $Mg_{17}Al_{12}$  (which has a melting point of approximately 460 °C, or 860 °F, and can exhibit soft at lower temperatures) does not contribute to fix the grain boundaries in alloys. The addition of 1% Calcium is a good solution to improve creep strength of Mg-Al alloys, but if the amount of Calcium excesses of 1%, wrought alloys will be very easy to obtain hot cracking. Moreover, low elastic modulus, limited cold workability and toughness, and susceptibility to corrosion are other disadvantages of existing Magnesium alloys. Consequently, the investigation and study of other alloys based on the Mg-Al system are of the most attention and interest so far to cater both commercial and industrial requirements.

The selected wrought alloy in simulations for this study was AZ31 (3 wt%Al, 1 wt%Zn), which is the exactly same one as in the industry "Double Hat "trail. AZ31 is one of the most popular magnesium extrusion alloys, and it is one of the main topics of the entire project. There are a lot of existing data found in literature, and then utilized as the foundation in this study. Luo and Sachdev [4] discussed properties and processing of AM30, one of the latest Mg alloys, and compared it with AZ31. They

stated that the increased zinc content in alloy AZ31 is the major difference between these alloys. Due to chemical composition change, the higher Zn alloy (AZ31) has higher strength at the expense of lower ductility. As a result of this, the expected extrudability of the alloy will most likely be lower. Table 1 shows chemical compositions for AZ31 and AM30 alloys.

**Table 1. Typical Chemical Compositions (wt%, bal Mg) For AZ31 and AM30 Alloys [5]**

<b>Alloy</b>	<b>Al</b>	<b>Mn</b>	<b>Zn</b>	<b>Fe</b>	<b>Ni</b>	<b>Cu</b>
<b>AZ31</b>	3.1	0.54	1.05	0.0035	0.0007	0.0008
<b>AM30</b>	3.4	0.33	0.16	0.0026	0.006	0.0008

### **1.3. Extrusion Welding**

Extrusion welding is a case of solid state bonding. In the process the surfaces of two solid bodies are brought into direct contact at elevated temperature and under pressure and then adhered to one another during forming of hollow shapes. The goal of this study is to develop a numerical model for extrusion welding of Magnesium alloy (AZ31) in DEFORM<sup>TM</sup> 2D and 3D to obtain the localized information at the extrusion welding seam and to predict weld integrity.

Extrusion welding taking place in hollow shapes and tubes can be basically divided into two general types, longitudinal welding and transverse welding known from billet to billet extrusion method where remaining part of a just extruded billet is welded to a new billet to be extruded. This project is focused on the longitudinal welding seams taking place during extrusion through a porthole die. A typical extrusion porthole die is presented in Figure 3.

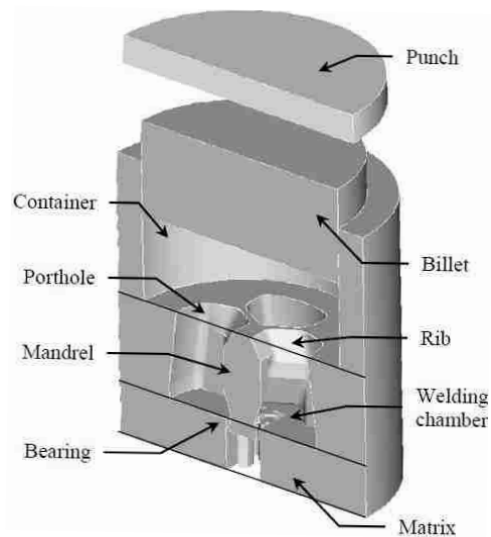


Figure 6. The porthole extrusion die [6]

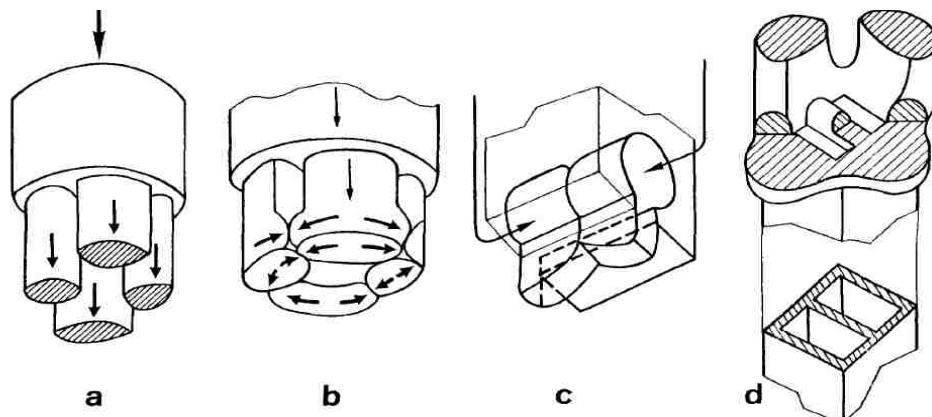


Figure 7. Steps in port-hold die extrusion. a: Forward extrusion; b: Sideways extrusion; c: Multiple voids filling; d: Extrudate completion [7]

According to Akeret [7], the longitudinal welding can be generally divided into four steps: 1. Forward extrusion, billet is divided into several smaller metal streams after goes through the ports of the die (Figure 4 a), 2. Sideways extrusion, streams are flowing tangentially into the spaces beneath the mandrel supports and then they contact each other (Figure 4 b), 3. Multi voids filling, if the extrusion shapes have



more than one void, another sideways extrusion step is required to fill the gaps between the several cores of one mandrel (Figure 4 c), 4. Extrudate completion, the hollow shape is extruded from the die. In terms of a successful extrusion welding, it takes place from the moment that streams touch with each other in step 3, until the involved surfaces are welded properly as a part of extrudate (Figure 4 d).

#### **1.4. Extrusion Welding Criteria**

The relationship between the quality of extrusion welding and extrusion temperature for three different heat treatments of 6xxx Aluminum alloy was reported in literature [8, 9]. Zasadzinski et. al. [8] as well as Chakkingal and Misiolek [9] concluded that there was no direct correlation between welding temperature and the extrudates' mechanical properties. The strength of welds increased but would be generally weaker than the other part of the extrudate after heat treatments. Liu et. al. [10] verified the role of the extrusion temperature and determined it not to be a critical process parameter. They also stated that the effective stress cannot be assumed as the only parameter to determine the quality of the extrusion welds. According to Donati and Tomesani [11], bending the extruded profiles and tearing the joints by inserting shaped wedges in the shape cavity are most commonly used methods to test the integrity of the extrusion welds. However, these destructive methods have a main disadvantage: they can only be utilized for dies which have been already manufactured thus representing a typical trial and error method. For this reason, the proposed criteria for welding quality prediction are of particular interest. Akeret proposed the maximum pressure criterion [7], Plata and Piwnik followed up with a modified criterion under

the assumption that the plastic deformation energy has the dominant effect on the welding quality [12]. The second criterion is employed in this work for data analysis and further verification.

The "Pressure-time" form of the Plata and Piwnik criterion is as following:

$$\int_t \frac{P}{\sigma} dt \geq COST \quad (1)$$

Where,  $t$  is the contact time,  $P$  is the normal pressure at the weld,  $\sigma$  is the effective stress and  $COST$  is a constant, which value assures sound extrusion welding. Donati and Tomesani [11, 13, 14], introduced speed as a correction factor to the criterion proposed by Plata and Piwnik. As a result of that, the "Pressure-time-flow" form of the Plata and Piwnik criterion has been created and has the following form:

$$\int_t \frac{P}{\sigma} dt \cdot v = \int_L \frac{P}{\sigma} dl \geq COST \quad (2)$$

Where,  $L$  is the path from the end point of the mandrel to the die exit. The  $COST$  item in equations (1 and 2) represents a threshold value to determine if the extrusion welding would take place. This value is varying because of different combinations of process parameters such as temperature, extrusion ratio (strain), ram speed (strain rate), as well as material properties such as flow stress and chemical composition.

## 1.5. Numerical Modeling and Simulation

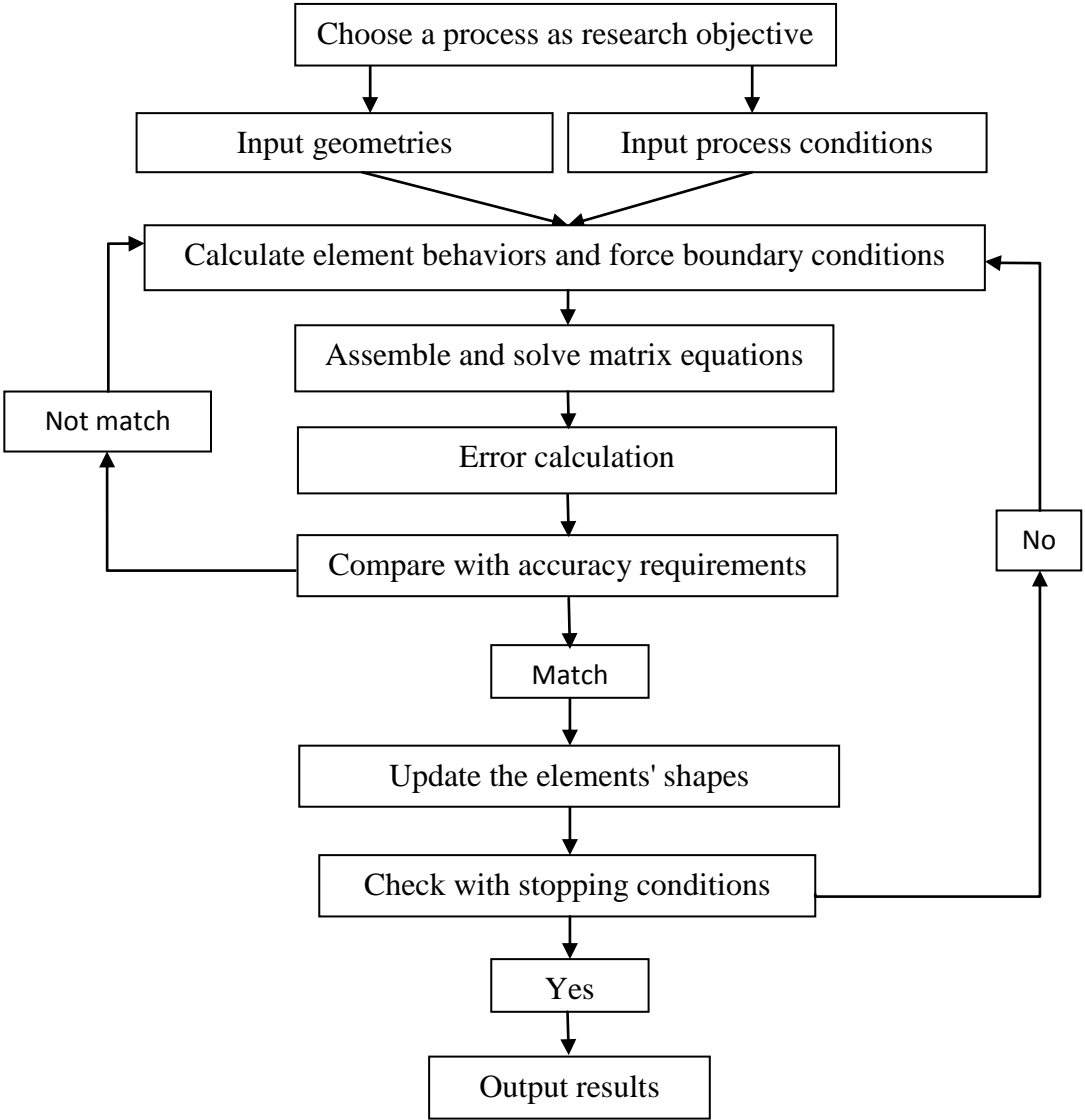
Throughout the history of extrusion technology, the development of this art was conducted experimentally or based on the empirical experiences of the tool designer or press operator. As a result, prototype tools and parts had to be tested repeatedly until an acceptable result was finalized. This methodology of extrusion improvement

contributed to a enormous amount of time and investment. To solve this problem, numerical modeling and simulation method is a perfect choice, because it can soundly express the certain practical process with mathematical equations or algorithm. Consequently, when implementation of new processing, tolerances, or alloys is involved, the modified process can be readily simulated and results also predictable.

Within this research project, the concept of numerical modeling is defined as the prediction of material response and micro-structural development with programs. The numerical simulation is the deformation process simulation utilized commercially available finite element modeling (FEM) software package, based on the numerical models.

Finite element modeling (FEM) (also known as finite element analysis (FEA)) achieves detailed visualization of elastic and/or plastic deformation for certain objectives. Extrusion is one of the typical metal forming processes, which involve the material and geometry nonlinearity, thus it has attracted great interest of FEM researchers. With the input of the detailed information about workpiece, tooling and boundary conditions, FEM can simulate how the materials respond during the entire extrusion process. After calculation, the distribution of temperatures, stresses, strains, velocities and displacements at each single step can be obtained comprehensively. Especially when FEM software is employed, the localized information is represented with vivid contour, plot as well as 2D even 3D graphs. FEM software provides very flexible simulation controlling options for the complexity of both modeling and analysis. Consequently, the proper approximation level and the associated

computational time can be managed simultaneously to meet the most engineering applications' requirements. The general FEM solution process is represented in the following flow chart:



Since the increasing interest and demand of FEM simulation for metal forming process, there are several industry-accepted FEM software packages, which are specialized in manufacturing process simulation are used widely nowadays, such as

LS-DYNA™, DEFORM™, QFORM™ .etc. With the consideration that this research work is concentrated in extrusion process, DEFORM™ package (including 2D and 3D versions) was chosen for this project due to its powerful function on metal deformation process simulation. This software is developed by Scientific Forming Technologies Corporation (SFTC). In the meantime, other benefits can be obtained from this choice [5, 15]: technical support via email, telephone, or web-conferencing; in-person training at SFTC and close collaboration with universities and research.

#### **1.6. Limited Capabilities of DEFORM™**

Despite of the fact that DEFORM™ is a leading industry-accepted metal deformation finite element method (FEM) software package and it has many advantages: relatively short time of computation, convenient importation and exportation of simulation variables and user-defined data for many materials, flexible edition of subroutines and very good capability of creating geometry [5]. It has a huge limitation of not only the recognition in terms of extrusion welding. Not only it cannot predict seam welding, but also cannot collect the local state variable information at the welded area. Figure 5 illustrates the welds (circled areas) in simulated extrusion welding. The metal streams contact each other in the welding chamber of the die, but flow as separate streams afterward instead of being bonded together. Because of this reason, the performed numerical simulation becomes not relevant to laboratory and industrial practices. Not only the modeling package does not predict welding to take place but also the simulation very often crushes in further steps. To overcome this

software limitation, a new modeling method has been proposed, and it is discussed in following parts of this paper.

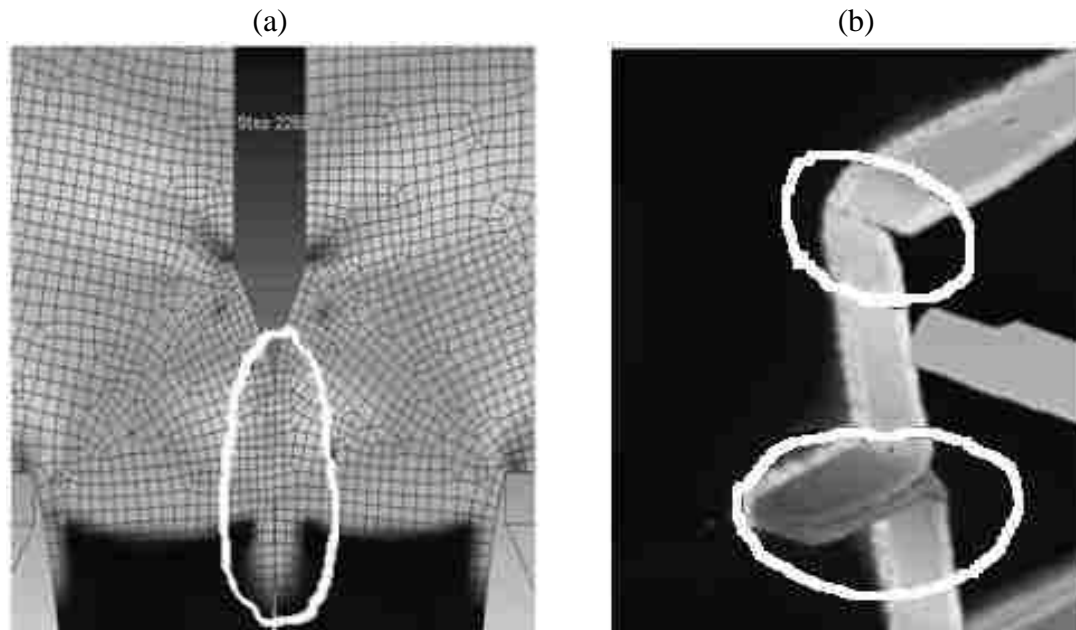


Figure 8. Extrusion welding seam in: (a) DEFORM™ 2D simulation and (b) [15] DEFORM™ 3D simulation

## 2. Physical Experiment and Numerical Simulation

### 2.1. “Double Hat ” Extrusion Industrial Trail

The numerical simulation was run in parallel to an industrial trail. The geometry of the extrudate was selected with crashworthiness studies in mind. Extruded profile is shown in Figure 6, and corresponding extrusion die is presented in Figure 7. During the extrusion process, the Mg alloy billet was divided into eight metal streams by the port-hole die and then welded together in the die welding chamber into “Double-Hat” shape.

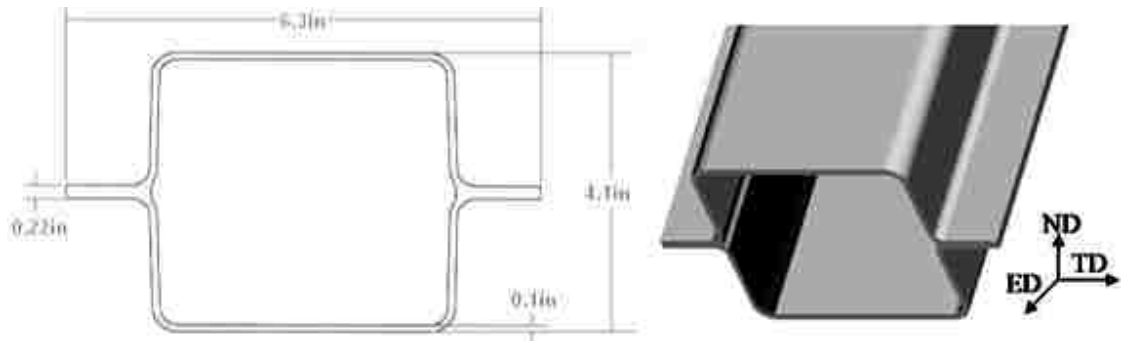


Figure 9. “ Double-Hat” extrudate. ED: Extrusion Direction, ND: Normal Direction, TD: Transverse Direction. [5]

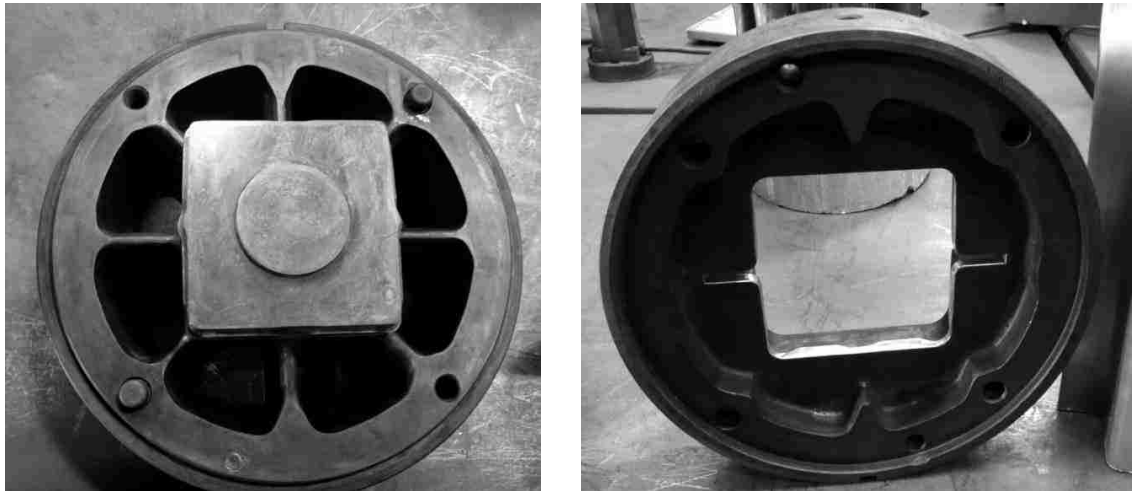


Figure 10. "Double Hat" extrusion die used in industrial trials

The details of the extrusion die are shown in Figure 7, while weld locations in the profile are marked in Figure 8. All the main settings and initial conditions of the extrusion industrial trail are presented in Table 2.

**Table 2. Extrusion Trail Process Parameters**

Initial Billet Temperature	538 °C (1000F)
Billet Diameter × Billet Length	200 mm (7.87 in) × 240 mm (9.45 in)
Extrusion Ratio	35.26
Upset Pressure	500 psi (3.45 MPa)
"Burp" Pressure	1500 psi (10.34 MPa)
Ram Speed	3.1 in/min (1.31 mm/s)
Extrusion Exit Speed	109.3 in/min (46.19 mm/s)
Press Capacity	1800 T ( $1.60 \times 10^7$ N)

The sound “Double Hat” extrudates were obtained in industrial trail. The extruded profile has a perfect design for the extrusion welding analysis, because it contains eight extrusion welding seams, which are marked in Figure 8 and called: middle, angle, and edge.

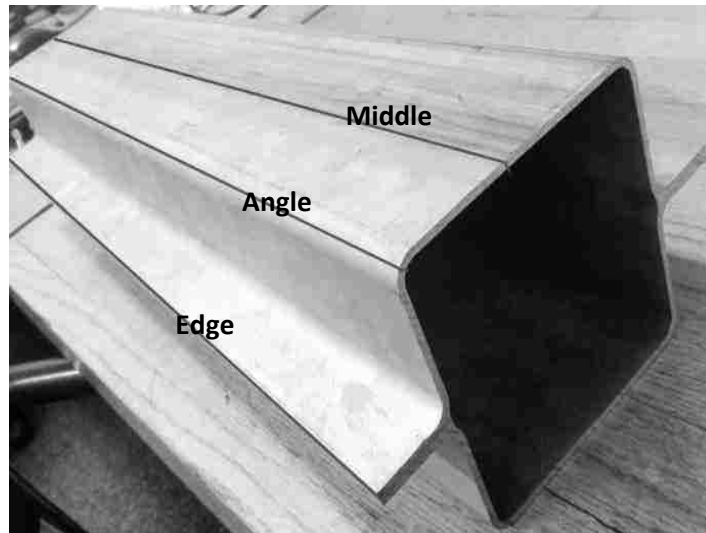


Figure 11. Location of welds within “Double Hat” profile



## 2.2. Numerical Simulation - DEFORM™ 2D

### 2.2.1. “Pressure Plate” Simulation Method

Middle weld of the "Double Hat" profile was selected due to its less complicated geometry and potential higher accuracy in performed analysis of the weld formation. As mentioned before, DEFORM™ package has a huge limitation when it is utilized to simulate extrusion welding. Consequently, a new simulation method called “Pressure Plate” has been developed to solve this dilemma. During this special simulation process, a metal plate with very small thickness was employed as a sensor and put in the location of extrusion welding. This “Pressure Plate” sensor performed as a data collector obtaining the local deformation information (temperature  $T$ , metal flow velocity  $v$ , normal pressure  $P$  and effective stress  $\sigma$ ) of the weld throughout the whole extrusion welding process.

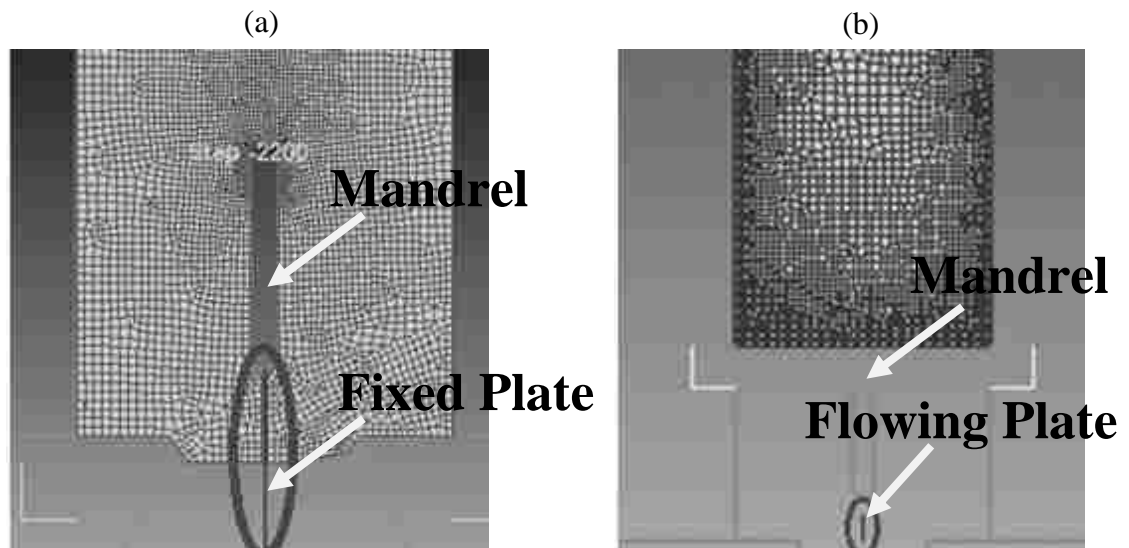


Figure 12. Pressure Plate in DEFORM™ 2D simulation: (a) Fixed Pressure Plate (b) Flowing Pressure Plate

Since the billet applies load on this pressure plate during the entire extrusion welding process hence it would experience applied stress and eventual deformation. The geometry and material of the Pressure Plate needs to be taken into account since it plays a critical role. The goal is also to guarantee the minimum disruption in metal flow during the entire simulation process.

**Table 3. Details for Two Types of the Pressure Plate**

Type Details	Fixed Pressure Plate	Flowing Pressure Plate
Dimensions	200mm(Length)×0.8mm (Thickness)	10mm(Length)×0.8mm (Thickness)
Material	1045 Steel	1045 Steel
Material model	Elastic	Elastic
Number of elements in FEM simulation	158	40

The Pressure Plate concept has been introduced in its two different forms (see Figure 9): the fixed plate and the flowing plate. As it is shown in Figure 9(a), the fixed pressure plate was localized below the mandrel as its extension, and its top part was fixed at the mandrel tip. During the simulation process, this pressure plate was

sandwiched between the metal streams in the exact position of a welding seam. The idea behind this type of pressure plate was to utilize it to record the localized parameters along the entire seam during the extrusion welding process. On the other hand, the flowing pressure plate (Figure 9(b)), named after its function, and was also introduced. This type of pressure plate was placed initially in the position where the metal streams begin to contact each other. The flowing plate is designed in such a way that it would flow with the metal streams through the entire length of the welding chamber of the die. The original idea behind this type of pressure plate was to record data for a specific point of the extrudate at the welding seam during the entire process. Since the flowing plate keeps track of a certain point of the weld as it moves with the extrudate, analysis of the collected data would be a useful method allowing studying the formation and development of the weld during the entire extrusion welding process.

**Table 4. Initial Settings for the DEFORM™ 2D Pressure Plate Simulation**

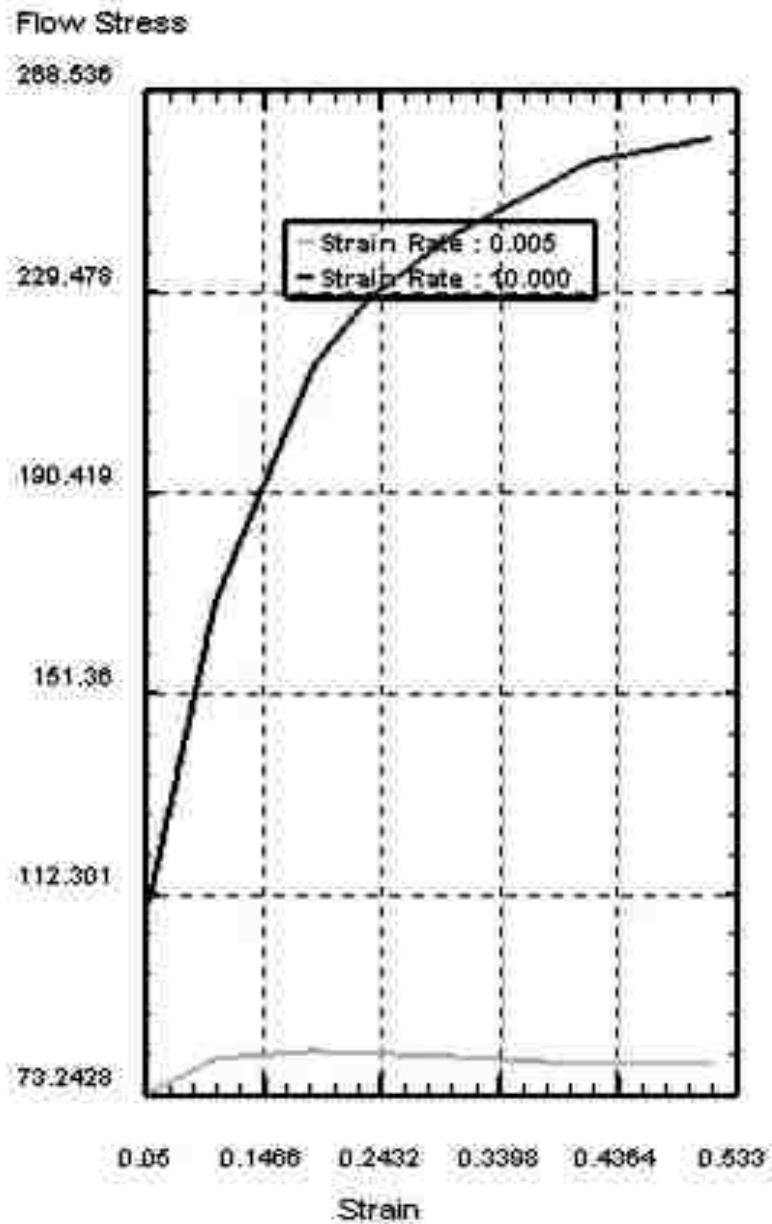
Billet Diameter x Billet Length	200 mm (7.87 in) x 240 mm (9.45 in)
Billet Temperature	538°C (1000°F)
Tooling Temperature	427°C (800°F)
Environment (Air) Temperature	20°C (68°F)
Shear Friction Coefficient (Billet – Billet)	0.7
Shear Friction Coefficient (Billet – Tooling)	0.2
Ram Speed	1.32 mm/s (0.052 in/s)
Heat Transfer Coefficient (Billet - Billet)	11000 W/(m <sup>2</sup> °C) (0.538 Btu/(s ft <sup>2</sup> °F))
Heat Transfer Coefficient (Billet - Tooling)	5000 W/(m <sup>2</sup> °C) (0.245 Btu/(s ft <sup>2</sup> °F))

The technical details about both pressure plates are shown in Table 3. The initial settings of DEFORM<sup>TM</sup> 2D for the simulation are presented in Table 4. The billet diameter, extrudate dimensions and billet and tooling temperatures were set to match the conditions of the industrial trail.

The AZ31 billet was treated as a plastic object in the performed simulations. The initial temperature was set at 538°C (1000°F) for the selected alloy, which is 85% - 89% of the 605 - 630 °C (1120 - 1170 °F) melting temperature range [5]. The material data, which have been imported into DEFORM<sup>TM</sup> package were originally found in Barnett and Lapovok's work [16, 17], and then supplemented with the data from Kuc and Pietrzyk at [18] and De Pari [5]. The flow stress curves for AZ31, presented in Figure 8, were generated by DEFORM<sup>TM</sup> and based on the imported flow stress data from literature and then applied into the simulations. The entire tooling (container, 8 port-hole die, and ram) employed in the simulations were modeled as rigid objects. As a result of this assumption there was no any deformation present during the entire extrusion process. Moreover, material selection for the Pressure Plate is another key issue throughout the entire simulation. In the very beginning of this study, there were two main material candidates: 1) 1045 steel, because of its generalized utilization and broad range of mechanical properties in both elastic and plastic region; and 2) AZ31 alloy, because of its identity with the billet material. However as shown in Figure 10, the material data for AZ31 are only valid for very limited strain range. Thus it was decided to use 1045 steel as a Pressure Plate material because of its known mechanical characteristics. The metal flow within the extrusion die as simulated in DEFORM<sup>TM</sup> 2D is shown in Figures 11, 12. The metal streams are not welded within the die as well

as after the extrudate exits the die. The performance of the “Pressure Plate” was observed and analyzed in several simulations. A conclusion was made that the sensor function of the Pressure Plate performed as designed during the entire extrusion welding process.

(a)



(b)

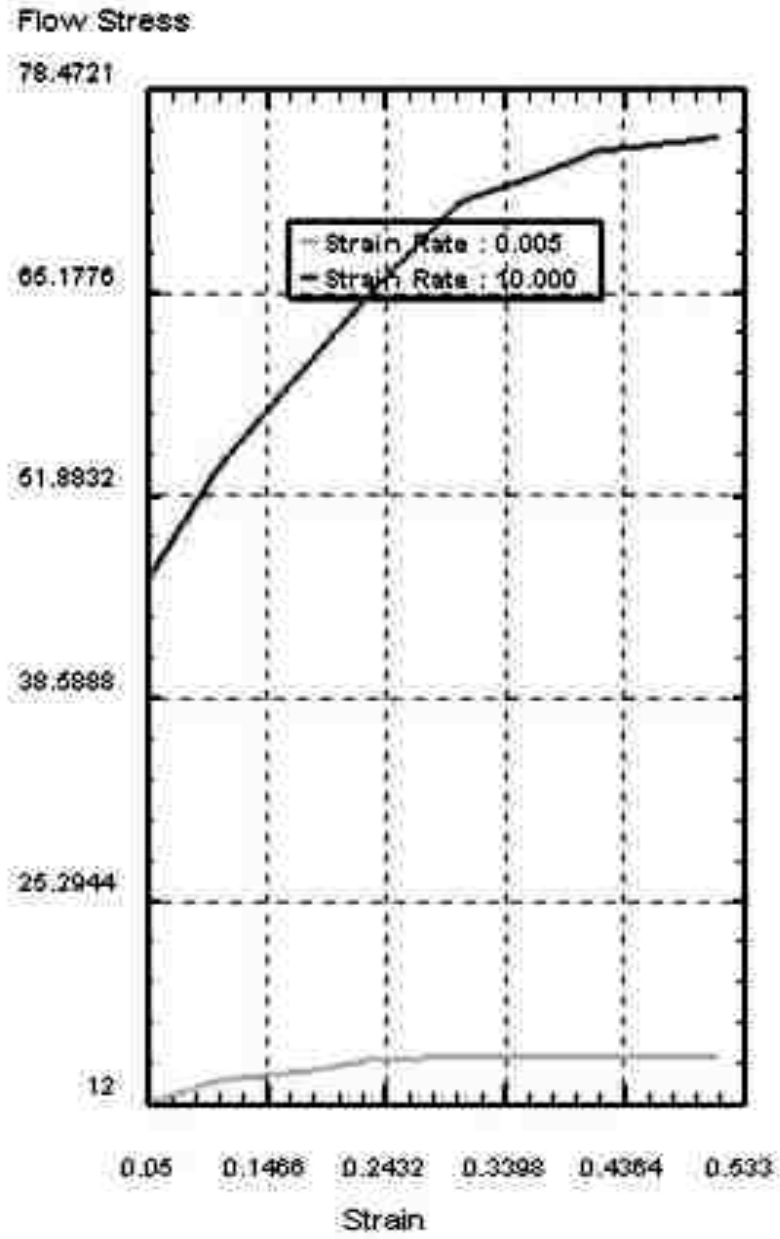


Figure 13. Flow stress curves of AZ31 alloy generated by DEFORM<sup>TM</sup> for: (a) 300°C and (b) 500°C

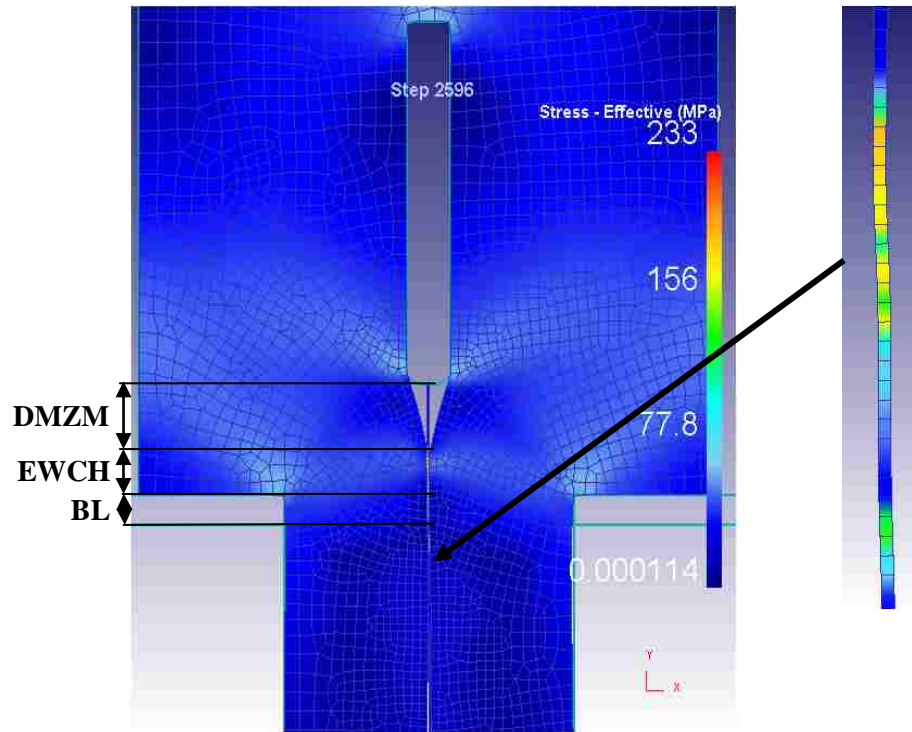


Figure 14. Fixed Pressure Plate simulation showing Effective Stress distribution. The marked regions are: dead metal zone behind mandrel (DMZM), effective welding chamber (EWCH) and bearing land of the die (BL).

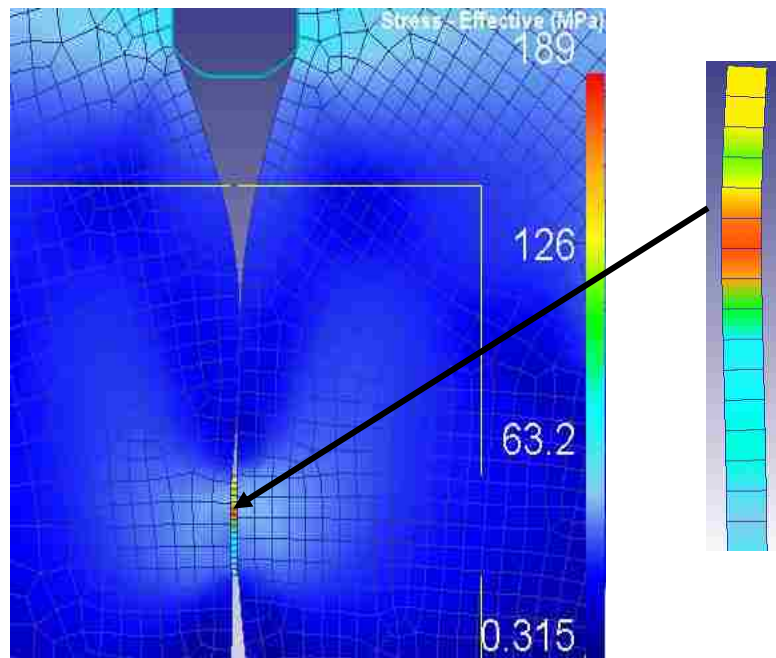


Figure 15. Flowing Pressure Plate simulation showing Effective Stress distribution

### 2.3. Numerical Simulation with DEFORM™ 3D.

The numerical simulations using DEFORM™ 2D were done as an initial step. Subsequently, another simulation of the “Double Hat” extrusion process has been established in DEFORM™ 3D in order to compare it with the 2D results. All of the initial settings were the same for DEFORM™ 2D and 3D simulations. In terms of material data, DEFORM™ package allows for exchange of material data entries between 2D and 3D versions of the software. Thus the AZ31 material data was imported from previous 2D simulation directly to new 3D models. The geometries and dimensions of all the objects (billet, container, ram, and 8 port-hole die) came from the extrusion industrial trail. In addition, since the “Pressure Plate” would be modeled in 3D and then localized in the expected position of the weld, the width of the plate was selected to be as the same value as the thickness of the extrudate. Figure 13 shows the general distribution of the effective stress for DEFORM™ 3D simulation.

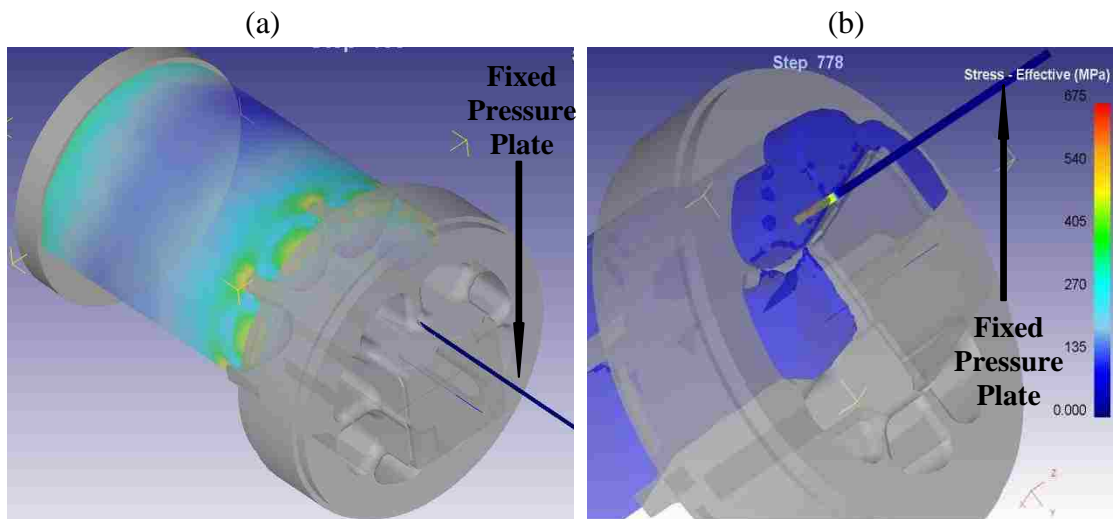


Figure 16. Extrusion simulation with Fixed Pressure Plate as marked with arrow in DEFORM™ 3D showing Effective Stress distribution: (a) Start of the simulation (b) Metal streams in contact with the fixed pressure plate.



### 3. Results and Analysis

#### 3.1. Validation of the Simulation Results

The FEM simulations are not error free due to model quality as well as certain process and material simplifications and approximations. Additionally, in order to achieve reasonable computing time the mesh size is very often compromised. Using basic calculation for the industrial trail parameters shown in Table 2, it was determined that the maximum possible stress is 534 MPa for the given extrusion billet and press size. These simple and approximate calculations give us reference range for performed numerical simulations.

#### 3.2. Result and Analysis of DEFORM™ 2D Simulation

According to the expression of Plata & Piwnik extrusion welding criterion, the effective stress, effective strain and normal pressure are three factors of the greatest importance for the quality of the extrusion weld. In DEFORM™ package, the effective stress is calculated as Von Mises stress by the following equations:

$$\bar{\sigma} = \sqrt{\frac{3}{2} \sigma'_{ij} \sigma'_{ij}} \quad (3)$$

$$\sigma'_{ij} = \sigma_{ij} - \delta_{ij} \sigma_{kk} / 3 \quad (4)$$

Where  $\bar{\sigma}$  is the flow stress,  $\sigma_{ij}$  is the stress component and  $\delta_{ij}$  is the Kronecker delta.

The strain rate is calculated by the following equation:

$$\dot{\epsilon}_{ij} = \frac{1}{2} (v_{i,j} + v_{j,i}) \quad (5)$$

Where  $\dot{\epsilon}_{ij}$  is the strain rate and  $v_{i,j}$  is the velocity component. Thus the effective strain (represented by  $\epsilon_{ij}$ ) is the time integral of strain rate:

$$\varepsilon_{ij} = \frac{1}{2} \int_t (v_{i,j} + v_{j,i}) dt \quad (6)$$

Moreover, the normal pressure is not calculated directly. It is obtained by dividing the nodal force by effective nodal area, which is based on adjoined element size.

### 3.2.1. Fixed Pressure Plate

Figures 14 and 15 show the results obtained from DEFORM<sup>TM</sup> 2D simulation of extrusion welding with fixed pressure plate. The localized parameters, such as effective stress, normal pressure, and effective strain were generated during simulation process. The X-axis is an extension of the mandrel along the extrusion direction. The marked regions in following figures are: dead metal zone behind mandrel (DMZM), effective welding chamber (EWCH) and the bearing land zone of the die (BL). One can easily notice that the maximum values for the effective stress and normal pressure (Figures 14 and 15) are taking place within the welding chamber before metal is flowing over the bearing land. It means that the metal streams divided by mandrel are then in contact with each other in this location, which is just behind the mandrel's dead metal zone (effective welding chamber (EWCH)). Subsequently, the metal streams are compressed together with increasing pressure until its maximum value. From this moment, extrusion weld is created, and strengthened within the die welding chamber. The most important is the fact that according to Plata and Piwnik criterion presented in equation (1) the Normal Pressure is mainly responsible for successful welding and graph in Figure 15 supports that.

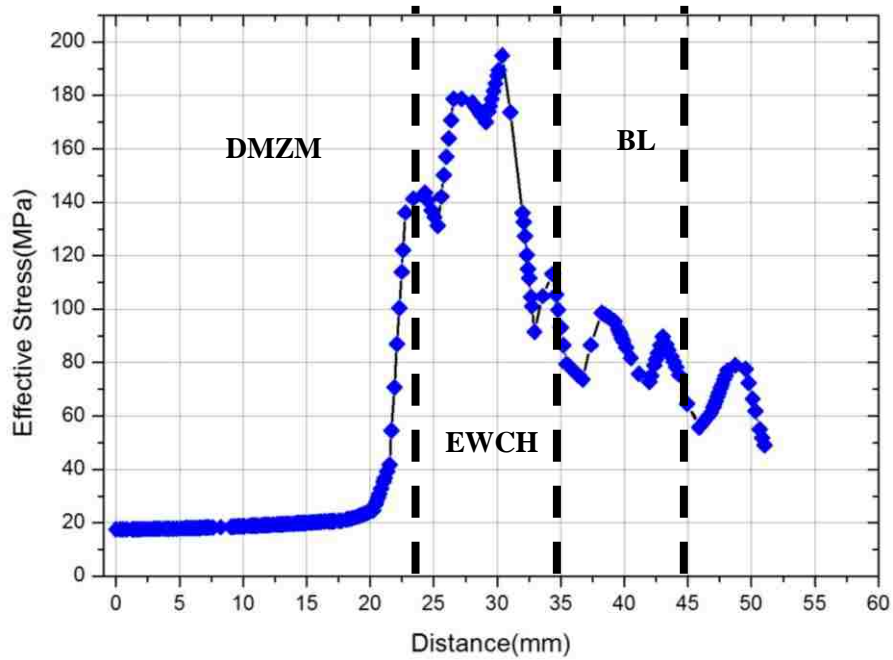


Figure 17. Effective Stress along extrusion weld with the increase of the distance to the bottom of mandrel. The marked regions represent: dead metal zone behind mandrel (DMZM), effective welding chamber (EWCH) and bearing land of the die (BL).

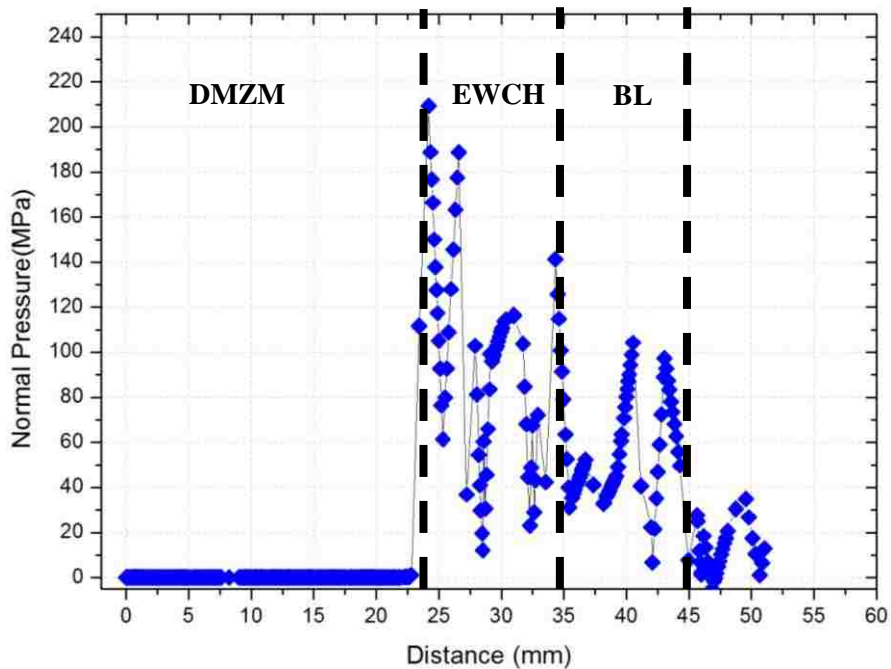


Figure 18. Normal Pressure along extrusion as the function of the distance to the bottom of mandrel. The marked regions represent: dead metal zone behind mandrel (DMZM), effective welding chamber (EWCH) and bearing land of the die (BL).

### 3.2.2. Flowing Pressure Plate

The extrusion welding simulation with the flowing pressure plate results obtained from DEFORM™ 2D are presented in Figures 16-21. As mentioned before, the flowing pressure plate was placed in the initial position where the metal streams begin to contact each other. It is also the end of the dead metal zone behind the mandrel. The collected data and generated values represent the localized effective stress and normal pressure. In Figures 16-21, X-axis represents the distance along extrusion direction from the mandrel tip to the position of flowing pressure plate. Based on the data in Figure 16, the time periods during which the flowing plate goes throughout the effective welding chamber (EWCH) and the bearing land of the die (BL) can be estimated as: 4 seconds for the EWCH and 4 seconds for the BL of the die.

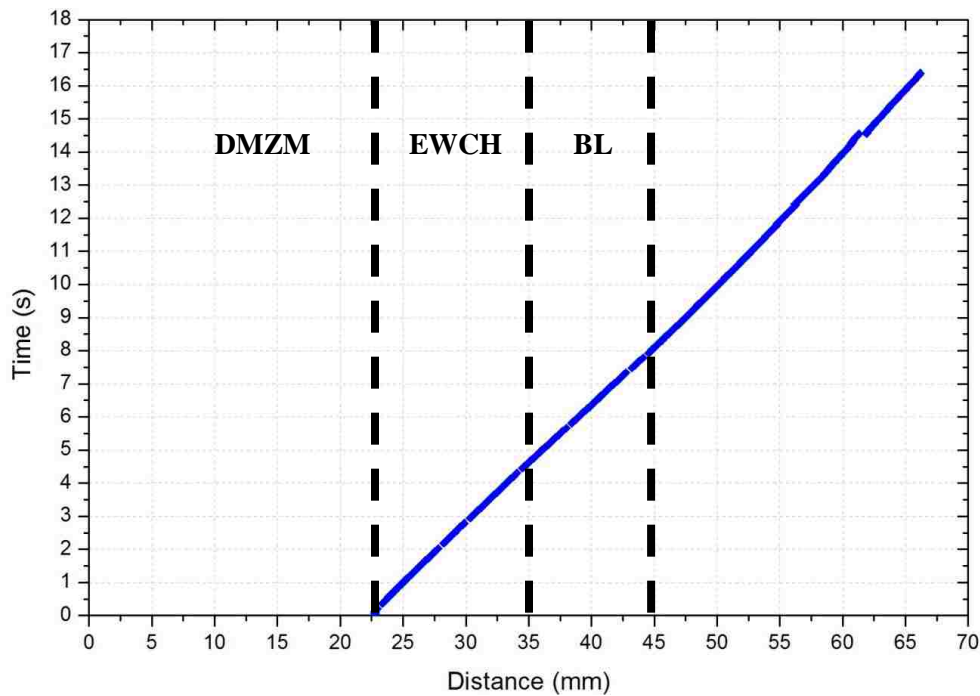


Figure 19. Time vs. displacement of the flowing pressure plate. The marked regions are: dead metal zone behind the mandrel (DMZM), effective welding chamber (EWCH) and bearing land of the die (BL).

The following Figures 17 and 19 are representing the distribution of effective stress and normal pressure at the flowing pressure plate. The fourth order polynomial curve fitting has been used to show the trend of the data and illustrated it by the solid lines in Figures 18 and 20. The polynomial used to fit the effective stress data is:

$$y = 1055.78 - 91.24x + 3.27x^2 - 0.05x^3 + 2.87 \times 10^{-4}x^4 \quad (7)$$

And the polynomial used to fit the normal pressure data is:

$$y = 441.80 - 27.85x + 0.82x^2 - 0.01x^3 + 5.65 \times 10^{-5}x^4 \quad (8)$$

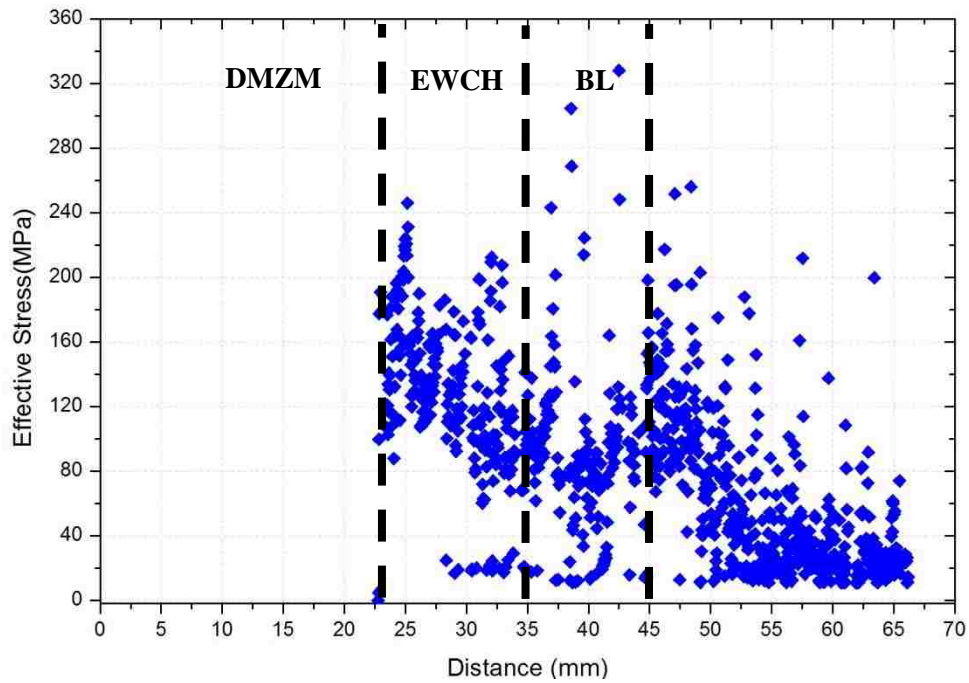


Figure 20. Effective stress data of the flowing pressure plate along extrusion weld as the function of the distance to the mandrel tip. Marked regions are: dead metal zone behind the mandrel (DMZM), effective welding chamber (EWCH) and bearing land of the die (BL).

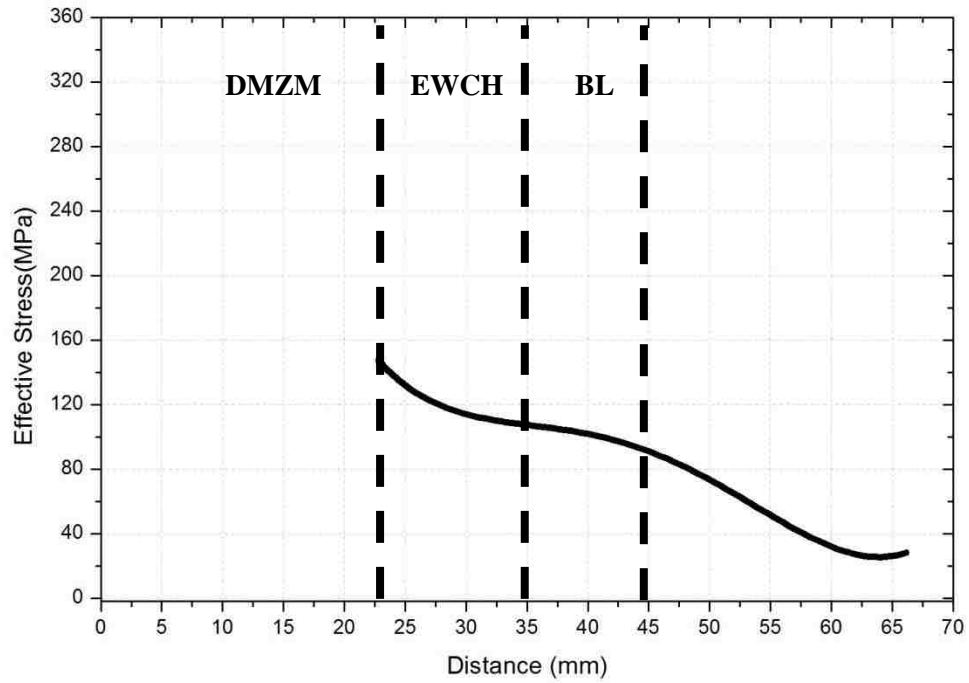


Figure 21. Polynomial curve fit of effective stress data of the flowing pressure plate. The marked regions are: dead metal zone behind the mandrel (DMZM), effective welding chamber (WCH) and bearing land of the die (BL).

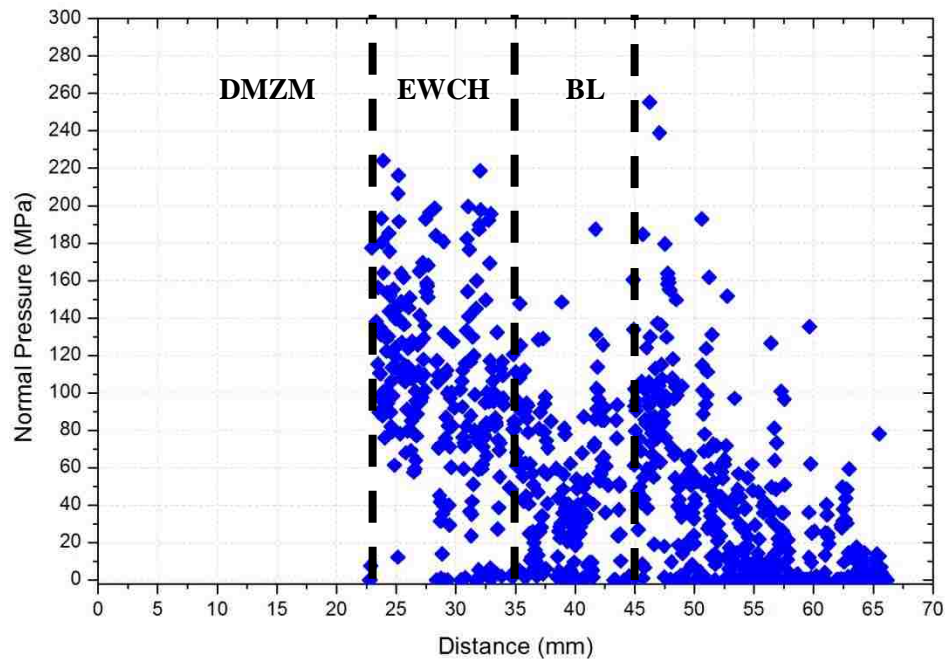


Figure 22. Normal Pressure data of the flowing pressure plate along extrusion weld as the function of the distance to the mandrel tip. The marked regions are: dead metal zone behind the mandrel (DMZM), effective welding chamber (EWCH) and bearing land of the die (BL).

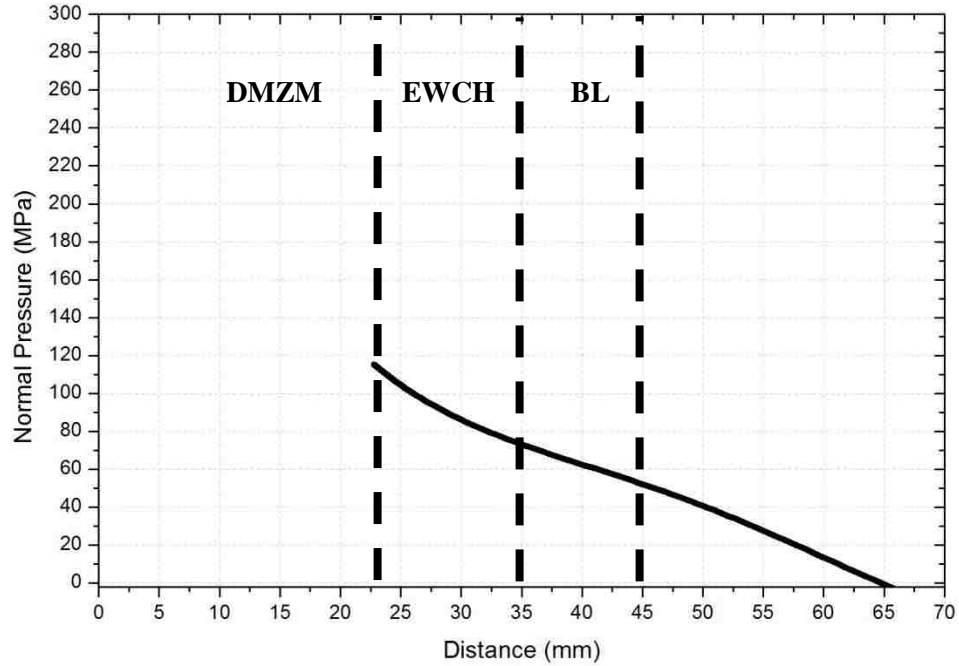


Figure 23. Polynomial curve fit of normal pressure data of the flowing pressure plate. The marked regions are: dead metal zone behind the mandrel (DMZM), effective welding chamber (EWCH) and bearing land of the die (BL).

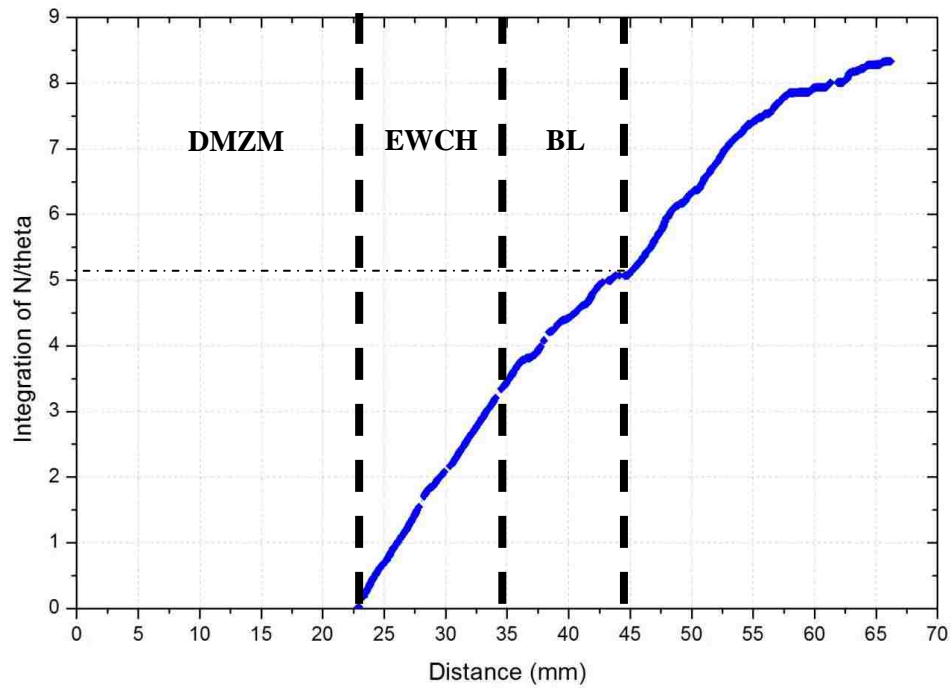


Figure 24. Integration of  $P/\sigma$  as the function of the distance to the mandrel tip. The marked regions are: dead metal zone behind the mandrel (DMZM), effective welding chamber (EWCH) and bearing land of the die (BL).

The time integration of  $\frac{P}{\sigma}$  term has been presented in Figure 21 according to the Plata & Piwnik criterion. Li et. al. also conclude in their work [19] that the ratio of the maximum normal pressure in the welding chamber to the effective stress on the welding plane relates directly to the quality of the longitudinal weld seams. This ratio remains almost constant along the whole length of the extrudate. This conclusion is validated partially by the graph in Figure 21 which shows an almost constant slope of the integration of the  $\frac{P}{\sigma}$  ratio. Consequently, the roughly estimated value of COST term in Plata & Piwnik criterion for extrusion welding can be read directly from Figure 21:

$$\int_t \frac{P}{\sigma} dt \geq \text{COST} = 5.2. \quad (9)$$

### 3.3. Result and Analysis of DEFORM™ 3D Simulation

The simulation with fixed pressure plate for extrusion welding has been successfully transferred into DEFORM™ 3D software. Figure 22 shows the distribution of effective stress on the pressure plate in the extrusion welding process. The arrow below the plate indicates the extrusion direction. The 3D fixed pressure plate was defined in the same way as in 2D. In Figure 22, the original point of the scale is the mandrel tip. In order to compare this result with the distribution represented with color scale, the effective stress data collected from the 3D fixed pressure plate is also shown in Figure 23.



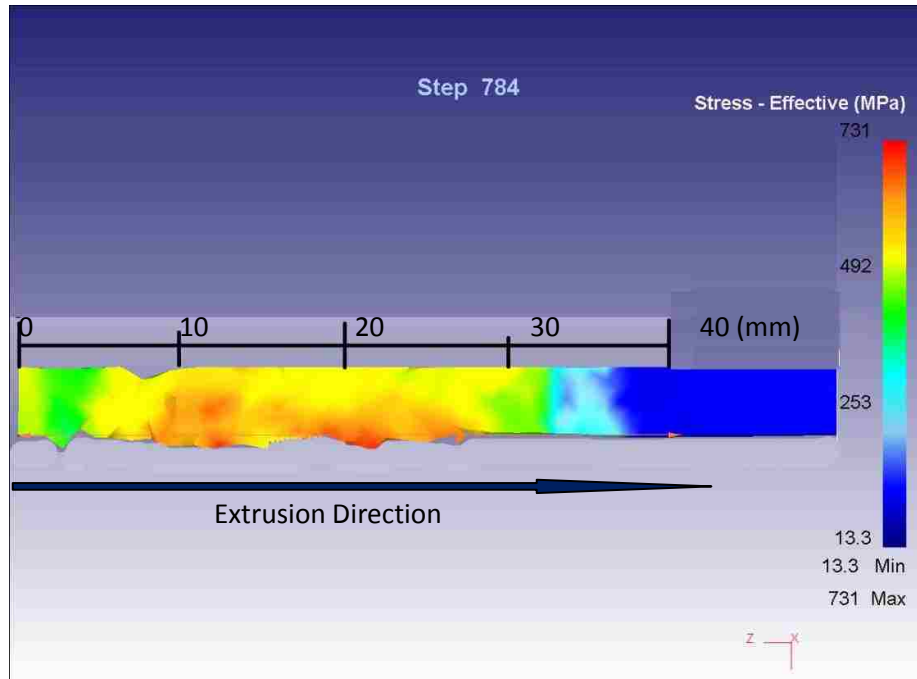


Figure 25. Distribution of effective stress on fixed pressure plate of DEFORM<sup>TM</sup> 3D simulation.

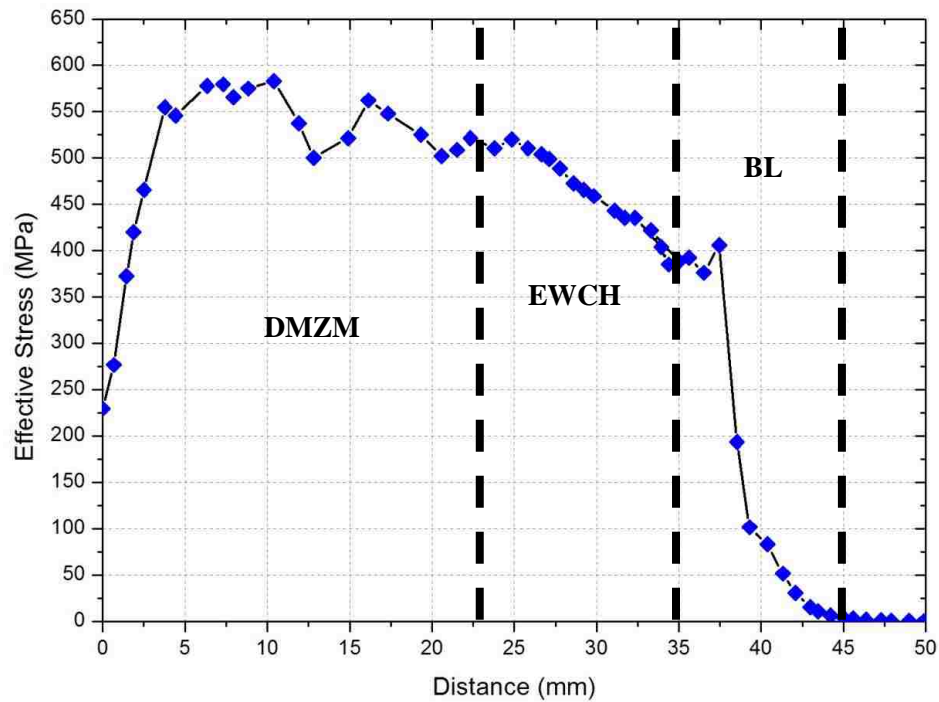


Figure 26. Effective stress data of the fixed pressure plate in DEFORM<sup>TM</sup> 3D simulation. The marked regions are: dead metal zone behind the mandrel (DMZM), effective welding chamber (EWCH) and bearing land of the die (BL).

After comparison with Figure 14, one can see that the results from the DEFORM<sup>TM</sup> 3D simulation do not agree with 2D results. Firstly, in the dead metal zone behind the mandrel (regions marked DMZM in Figures 14 and 23) the value is close to zero in 2D result but not in 3D. There is no contact between metal streams and the pressure plate in this region, thus the 2D results seem reasonable. On the other hand, the possible reason for the unexpected part of 3D result is that, within this 3D simulation for the fixed pressure plate, the pressure plate was placed in the very beginning of the extrusion process before it reached the steady state. Secondly, the data collected from 3D simulation are very different than from 2D simulation. This is because the 3D simulation in this work represents the entire "double hat" extrusion but the 2D simulation is only modeling single weld. Thirdly, the other trends of the data of the 3D simulation agree with 2D. Thus in general, the Pressure Plate method can be employed in DEFORM<sup>TM</sup> 3D but needs further analysis and modifications.

#### **4. Conclusion**

In this study, the conditions from industrial extrusion trail have been employed into numerical simulation to verify Plata and Piwnik extrusion welding criterion. The material data from as-cast homogenized AZ31 compression test flow stress have been collected from literature and employed into both 2D and 3D modeling. Based on the performed simulations the following conclusions can be made from the effort of this work:

- 1) DEFORM<sup>TM</sup> package has been successfully utilized into the simulation of extrusion welding. The proposed method allows analysis of extrusion welding in both 2D and 3D versions for specific Magnesium profile.
- 2) Two kinds of pressure plates, the fixed pressure plate and flowing pressure plate, have been defined as sensor and applied into DEFORM<sup>TM</sup> simulations.
- 3) In DEFORM<sup>TM</sup> 2D simulation, both fixed and flowing pressure plate simulation method have been achieved successfully. Showing location for maximum Normal Pressure, which according to Plata and Piwnik is responsible for successful extrusion welding.
- 4) The effective welding chamber has been found and marked as the region where extrusion welding mainly takes place.
- 5) Obtained simulation results can be used to optimize extrusion die design.

## **5. Future Work**

This simulation is very meaningful for practical extrusion die design. The geometry and dimension of the welding chamber are always critical issues in the extrusion die manufacturing industry. Thus these kinds of numerical simulations, which were applied not only within the die but also for the entire extrusion welding process are good starting point for modification and optimization for extrusion die designing and consequently for the extrusion process. Although some results have been obtained, a lot of future work is still very necessary including:

- 1) Additional physical experiments of extrusion welding for Magnesium alloys need to be performed. In this study, the foundation of performed simulations is the successful industrial trail of "Double Hat" extrusion for AZ31. It is far from enough to support a complete analysis sufficiently. Further physical verification could be developed on the basis of the presented simulations in this thesis. The observation and analysis should not only focus on the extrudate, which has left the die, but also on the material in deformed billet flowing into the die..
- 2) There is a need for more material data. IN this study, the material data entries input into FEM software were collected from literature. Currently, there s a lot of relative research being done using compression test and torsion test, which examine the characteristics of Magnesium alloys. The refined material information entries into software packages result in increased accuracy and reliability.
- 3) DEFORM<sup>TM</sup> 3D simulation still needs modification. A possible solution is the user defined subroutine. DEFORM<sup>TM</sup> package supplies user defined option for most simulation settings, for example the material information, equations for calculation, as well as the values of constants. The plate which has been applied into DEFORM<sup>TM</sup> 3D simulations is much smaller than the workpiece. Thus the huge difference in size between the elements in workpiece and plate is the main reason why the 3D simulation obtained sometimes unreasonable results. For future work, an algorithm should be developed and implemented

into DEFORM™ software to modify the mesh of localized elements and/or selected calculation procedures of the simulations.

## 6. References

- [1] M. Bauser, G. Sauser, K. Siegert, *Extrusion*, Second Edition, ASM International, 2006
- [2] W. Z. Misiolek, *Extrusion Excellence: Applied Fundamentals for Aluminum Extruders*, Atlanta, Georgia, February 18, 2009.
- [3] M. M. Avedesian, H. Baker, *Magnesium and Magnesium Alloys (ASM Specialty Handbook)*, illustrated edition, June 1, 1999.
- [4] A. A. Luo and A. K. Sachdev, Development of a new wrought magnesium-aluminum-manganese alloy AM30, *Metallurgical and Materials Transactions A: Physical Metallurgy and Materials Science* 2007, Vol. 38A, 1184-1192.
- [5] L. De Pari Jr., W. Z. Misiolek, J.H. Forsmark, A. A. Luo, Flow stress numerical modeling for large strain deformation in Magnesium alloy AZ31, *Computer Methods in Materials Science*, Vol. 10, 2010, No. 2.
- [6] Elisabetta Ceretti and Claudio Giardini, Developmnet and implementation of an algorithm for the simulation of material welding in extrusion process, *First International Conference on Sustainable Manufacturing*, October 17-18, 2007.
- [7] R. Akeret, Extrusion welds—quality aspects are now center stage, *Proceeding of 5th international aluminum extrusion technology seminar*, Chicago, IL, Vol. I, 1992, 319-336, Aluminum extruder council and the aluminum association.
- [8] J. Zasadzinski, J. Richert, and W. Z. Misiolek, Weld quality in extruded Aluminum hollow sections, *Light Metal Age*, Vol. 51, 1993, 3&4, 8-13.
- [9] U. Chakkingal and W. Z. Misiolek, *Welding phenomena in extruded Aluminum hollow profiles*, TMS, February, 1998.
- [10] G. Liu, J. Zhou, J. Duszczuk, FE analysis of metal flow and weld seam formation in a porthole die during the extrusion of a magnesium alloy into a square tybe and the effec of ram speed on weld strength, *Journal of materials processing technology*, 200, 2008, 185-198.
- [11] L. Donati, L. Tomesani, The prediction of seam weld quality in aluminum extrusion, *J. Mater. Process. Technol.* 153/154 (2004) 366–373.
- [12] M. Plata, J. Piwnik, Theoretical and experimental analysis of seam weld formation in hot extrusion of aluminum alloys, *Proceedings of Seventh International Aluminum Extrusion Technology Seminar ET*, vol. I, 2000, 205–211.
- [13] L. Donati, L. Tomesani, Analysis of material flow and welding in aluminum extrusion of hollow sections, in: *V AITEM Conference*, Bari, September 2001, 678–688.
- [14] L. Donati, L. Tomesani, Simulation of Welding Conditions in Porthole Die Extrusion, *AMST (Udine), Advanced Manufacturing Systems and Technology*, July 2002, 437.
- [15] L. De Pari Jr., Private Communication.

- [16] Barnett, M. R., Z. Keshavarz, et al., Influence of grain size on the compressive deformation of wrought Mg-3Al-1Zn, *Acta Materialia*, 2004, 52(17): 5093-5103.
- [17] Lapovok, R. Y., M. R. Barnett, et al., Construction of extrusion limit diagram for AZ31 magnesium alloy by FE simulation, *Journal of Materials Processing Technology*, 2004, 146(3): 408-414.
- [18] D. Kuc, M. Pietrzyk, Physical and Numerical Modeling of Plastic Deformation of Magnesium Alloys: *Computer Method in Materials Science*. Vol. 10, 2010, No. 2, 130-141.
- [19] L. Li, H. Zhang, J. Zhou, J. Duszczyk, G.Y. Li, Z.H. Zhong, Numerical and experimental study on the extrusion through a porthole die to produce a hollow magnesium profile with longitudinal weld seams, *Material and Design*, 29, 2008, 1190-1198.

## **7. VITA**

Yan Xu was born on October 23, 1985 in Beijing, China. After graduated from Beijing No. 4 High School, he began his undergraduate education in Beijing University of Technology (BJUT) with an interest in Mechanical Engineering. During undergraduate study, he participate the project of The Design of High-speed Spindle Dynamic Balancing Control System Based on Digital Signal Processing (DSP) in July, 2006. In September, 2007 he joined the research group of YCHSQ-1 Permanent Magnet Type Retarder and finished the simulation and optimization part under the guidance of Professor Yunkang Sui, who was also his advisor during undergraduate study.

In the senior year (2008), Yan Xu went to Georg-Simon-Ohm-Hochschule Nuremberg, Germany to finish his thesis of Bachelor of Science degree. During the half year in Germany, he finished the project on Finite Element Analysis and Optimization of a Light-Weight Bracket under the guidance of Prof. Dr. Martin Ertz. In addition, he obtained not only meaningful academic experience from the project but also had a very wonderful time in Europe. He graduated from Beijing University of Technology (BJUT) with Bachelor of Science degree after the completion of his thesis in Germany.

In August, 2008 Yan Xu was enrolled in PhD program by Mechanical Engineering and Mechanics Department of Lehigh University. He joined Institute for Metal Forming in 2009 and began to work on the project on Numerical Modeling of Extrusion Welding in Magnesium Alloys.